# Fast Flavor Depolarization of Supernova Neutrinos

Soumya Bhattacharyya[*] and Basudeb Dasgupta[†]

*Tata Institute of Fundamental Research, Homi Bhabha Road, Mumbai, 400005, India*

Flavor-dependent neutrino emission is critical to the evolution of a supernova and its neutrino signal. In the dense anisotropic interior of the star, neutrino-neutrino forward scattering can lead to fast collective neutrino oscillations, which has striking consequences. We present a theory of fast flavor depolarization, explaining how neutrino flavor differences become smaller, i.e., depolarize, due to diffusion to smaller angular scales. We show that transverse relaxation determines the epoch of this irreversible depolarization. We give a method to compute the depolarized fluxes, presenting an explicit formula for simple initial conditions, which can be a crucial input for supernova theory and neutrino phenomenology.

Metronomes sway in lockstep, crickets chirp in a chorus, and neurons fire in sync—all examples of coordinated action by seemingly unregulated agents [1]. Neutrinos emitted by collapsing stars can also exhibit such collective behavior in their quantum mechanical flavor oscillations [2–23]. Astonishingly, this dense gas of neutrinos can change its flavor at a rate proportional to the neutrino density [24–39], much faster than any individual neutrino. It is as if a marching band outruns Usain Bolt. Such fast evolution may erase the differences between neutrino fluxes, i.e., depolarize in flavor, within picoseconds and over distances smaller than a pinhead. In this Letter, we propose a theory of "fast flavor depolarization," which has major consequences for supernova (SN) explosions and their signals at neutrino telescopes.

Fast oscillations are a peculiar avatar of neutrino oscillation. They involve pairwise $\nu_e\bar{\nu}_e \leftrightarrow \nu_{\mu,\tau}\bar{\nu}_{\mu,\tau}$ conversions [24–29] that proceed at a rate $\sqrt{2}G_F n_\nu \sim 10$ cm$^{-1}$, proportional to the local neutrino density $\sim (10^{35}$–$10^{30})$ cm$^{-3}$ at radii $r \sim (10$–$100)$ km in a SN [40]. This rate greatly exceeds the oscillation rate in vacuum $\omega = |\Delta m^2|/(2E) \sim$ km$^{-1}$. (We use $\hbar = c = 1$, expressing everything in units of length or time.) As such, fast oscillation is quite insensitive to the size or sign of the neutrino-mass-square difference $\Delta m^2$, and stems from an *instability* that can be triggered by any nonzero $\omega$ [27].

Neutrino distributions, $F_\alpha[\vec{p}] = d^3 n_\alpha/d^3 \vec{p}$, vary with direction in a flavor-dependent manner. Here $\alpha = \overset{(-)}{\nu}_{e,\mu,\tau}$. If the $\nu_{\mu,\tau}$ and $\bar{\nu}_{\mu,\tau}$ flavors are almost identical (hereafter denoted as $\nu_x$), as motivated by the much lower $\mu^\pm$ and $\tau^\pm$

densities than those of $e^\pm$, the criterion for instability is met if the $\nu_e$ and $\bar{\nu}_e$ distributions are equal along some direction (s) [27–39]. Figure 1 shows a sketch of the decoupling region in the SN. The different neutrino flavors have hierarchical interaction rates, and they kinetically decouple at $R_{\nu_e} > R_{\bar{\nu}_e} > R_{\nu_x}$. In the decoupling region, this can produce relative forward excesses in the fluxes of $\nu_x$ over $\bar{\nu}_e$, and $\bar{\nu}_e$ over $\nu_e$ [41–45], as shown in the schematic polar plots. This allows the $\nu_e$ and $\bar{\nu}_e$ distributions to develop a *crossing*, as believed to be required for the fast instability.

Although the triggering and initial growth of fast oscillations are well understood [24–39], owing to complicated nonlinear evolution [31,35,39] the final impact is not yet known. Stellar explosion and the neutrino signal are sensitive to the nonlinearly processed flavor-dependent fluxes, and the required neutrino theory prediction of these fluxes is lacking. In this work, we address this crucial theoretical and phenomenological obstacle and pave a clear path forward. We present a theory that explains *how, when,*
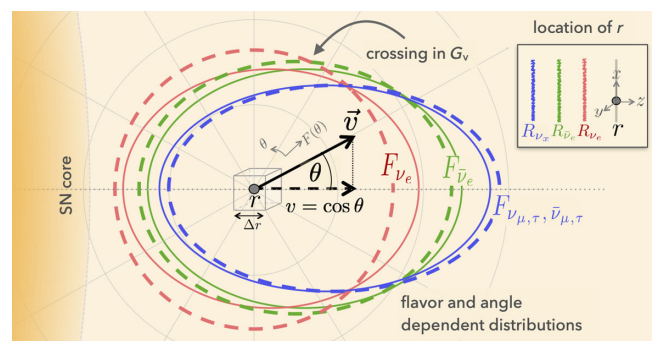


FIG. 1. Schematic: SN neutrino decoupling, just above $R_\alpha$, with illustrative polar plots of angle-dependent neutrino distributions $F_\alpha$, initially (thick dashed ellipses) with a forward excess of $\bar{\nu}_e$ (green) over $\nu_e$ (red), producing a *crossing*, and of $\nu_x$ (blue) over $\bar{\nu}_e$, and, finally (thin ellipses) their differences reduced due to depolarization.
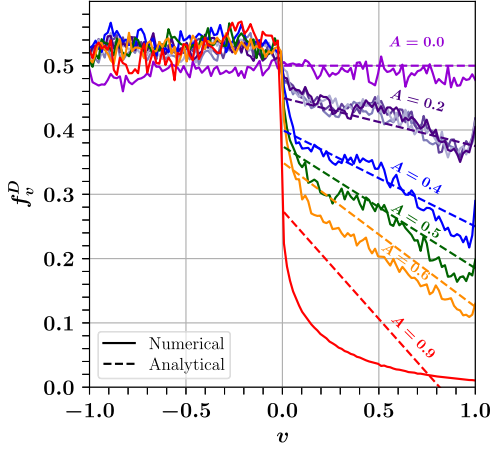
FIG. 2. Depolarization factor: Analytical (dashed) and numerical (solid) results for coarse-grained $f_v^D$, as a function of the radial velocity, $v = \cos\theta$, for different initial neutrino ELNs labeled by their lepton asymmetry $A$. For $A = 0.2$, the different purple lines are for different initial seeds.

and *to what extent* do the flavor differences change due to fast oscillations.

For two flavors, say $e$ and $\mu$, the final distributions after depolarization can be written as

$$F^{\text{fin}}_{\overset{(-)}{\nu}_e,\overset{(-)}{\nu}_\mu}[\vec{p}] = (1 - f_{\vec{p}}^D)F^{\text{ini}}_{\overset{(-)}{\nu}_e,\overset{(-)}{\nu}_\mu}[\vec{p}] + f_{\vec{p}}^D F^{\text{ini}}_{\overset{(-)}{\nu}_\mu,\overset{(-)}{\nu}_e}[\vec{p}], \quad (1)$$

where the depolarization factor $f_{\vec{p}}^D$, which is the same for $\nu$ and $\bar{\nu}$, is equal to $\frac{1}{2}$ for perfect equality of distributions and 0 for no change. Values between $\frac{1}{2}$ and 1 indicate effective flavor conversion. We will present an explicit formula for $f_v^D$ [in Eq. (7)], assuming an azimuth-symmetric $F$. This result for $f_v^D$ is previewed in Fig. 2. As predicted analytically, the extent of depolarization depends on the radial velocity $v = \cos\theta$ and lepton asymmetry $A \propto (n_{\nu_e} - n_{\bar{\nu}_e})$. In the following, we set up the problem, present our theory that leads to this result, and conclude by discussing the relevance of our results to SN physics and neutrino phenomenology.

*Setup and notation.*—As shown in Fig. 1, we consider a small region of size $\Delta r$ around $r$, just outside radii $R_\alpha$ in a SN where $\mathcal{O}(G_F^2)$ momentum-changing collisions have ceased. In a realistic SN, $R_\alpha \sim$ km and $(r - R_\alpha) \ll R_\alpha$. The equation for a two-flavor $|\nu\rangle$ with energy-momentum $(E, \vec{p})$, in a spacetime volume where all macroscopic parameters such as density $n$ are constant, is [27,28,36,39]

$$(\partial_t + \vec{v}.\vec{\nabla})\mathsf{S}_{\omega,\vec{v}} = (\mathsf{H}_\omega^{\text{vac}} + \mathsf{H}^{\text{mat}} + \mathsf{H}_{\vec{v}}^{\text{self}}) \times \mathsf{S}_{\omega,\vec{v}}. \quad (2)$$

Antineutrinos are represented with $\omega = -|\Delta m^2|/(2E)$, extending $\omega$ to negative values. Sans-serif letters denote vectors in flavor space, whose magnitudes are shown in the usual font. E.g., $\mathsf{S}_{\omega,\vec{v}}[\vec{r}, t]$, with $|\mathsf{S}_{\omega,\vec{v}}| \equiv S_{\omega,\vec{v}} = 1$, is the normalized Bloch vector corresponding to the density

matrix $|\nu_{\omega,\vec{v}}\rangle\langle\nu_{\omega,\vec{v}}|$ varying in $(\vec{r}, t)$. We work in the flavor basis $\{\hat{\mathbf{e}}_1, \hat{\mathbf{e}}_2, \hat{\mathbf{e}}_3\}$, where the longitudinal component along $\hat{\mathbf{e}}_3$ is denoted by $(\cdot)^\parallel$ and the transverse by $(\cdot)^\perp$. Thus, $\mathsf{S}^\parallel$ encodes the flavor composition $|\langle\nu_e|\nu\rangle|^2 - |\langle\nu_\mu|\nu\rangle|^2$. Note that $\mathsf{S}^\parallel$ can be negative, but not $S^\parallel = |\mathsf{S}^\parallel|$. The vector $\mathsf{H}_\omega^{\text{vac}} = \omega(\sin 2\vartheta, 0, \cos 2\vartheta)$ causes oscillations in vacuum, $\mathsf{H}^{\text{mat}} = \sqrt{2}G_F(n_{e^-} - n_{e^+})(0, 0, 1)$ gives matter effects, and $\mathsf{H}_{\vec{v}}^{\text{self}} = \int d^3\vec{p}'_{\omega',\vec{v}'}/(2\pi)^3 g_{\omega',\vec{v}'}(1 - \vec{v} \cdot \vec{v}')\mathsf{S}_{\omega',\vec{v}'}$, with $g_{\omega,\vec{v}} = (F_{\nu_e} - F_{\nu_\mu})$ for $\omega > 0$ and $(F_{\bar{\nu}_\mu} - F_{\bar{\nu}_e})$ for $\omega < 0$, causes collective effects.

In the fast oscillation limit, we neglect the $\mathsf{H}_\omega^{\text{vac}}$ and $\mathsf{H}^{\text{mat}}$ in Eq. (2), compared to $\mathsf{H}_{\vec{v}}^{\text{self}}$. The self-term then enters the Hamiltonian only through the difference of distributions integrated over $\omega$ [27], defined by the electron lepton number (ELN) distribution $G_{\vec{v}} = \int_{-\infty}^{+\infty} d\omega g_{\omega,\vec{v}}$, and the equation for $\mathsf{S}_{\omega,\vec{v}}$ becomes essentially $\omega$ independent. For locally azimuth-symmetric ELNs, Eq. (2) becomes

$$(\partial_t + v\partial_z)\mathsf{S}_v = \mu_0 \int_{-1}^{+1} dv' G_{v'}(1 - vv')\mathsf{S}_{v'} \times \mathsf{S}_v, \quad (3)$$

where $v$ is the radial velocity and $\mu_0$ is the collective potential. Initial conditions are $\mathsf{S}_{\omega,\vec{v}}|^{\text{ini}} = +\hat{\mathbf{e}}_3$ and Eq. (3) is the same for all $\omega$, so $\nu$ and $\bar{\nu}$ have identical solutions. In our algebra, hereafter, $t = \mu_0 t$ and $z = \mu_0 z$, which are dimensionless. For concreteness, ELNs are taken to be piecewise constant with one crossing at $v = 0$,

$$G_v = \begin{cases} 1, & \text{if } v > 0, \\ A - 1, & \text{if } v < 0, \end{cases} \quad (4)$$

and the lepton asymmetry $A = \int_{-1}^{+1} dv G_v$ takes values in $\{0.0, 0.2, 0.4, 0.5, 0.6, 0.9\}$. For our numerical examples, we solve Eq. (3) with $\mu_0 = 33$ cm$^{-1}$, corresponding to $n_\nu \approx 5 \times 10^{33}$ cm$^{-3}$. Periodic boundary conditions are assumed on $z \in \Delta r = (-1.5, +1.5)$ cm, treating this "box" as a part of a larger system. In lieu of $\mathsf{H}_\omega^{\text{vac}}$, the $\mathsf{S}_v^\perp[z, t = 0]$ are explicitly seeded with amplitude $10^{-6}$ to start the flavor evolution. This choice plays a negligible role in deciding the final state; see the Supplemental Material [46] for more details. The numerical methods are the same as in Ref. [39].

*Multipole diffusion.*—We define $\mathsf{M}_n = \int_{-1}^{+1} dv G_v L_n \mathsf{S}_v$ as the $n$th moment of $\mathsf{S}_v$, with $L_n[v]$ being the $n$th Legendre polynomial in $v$. In terms of $\mathsf{M}_n$, Eq. (3) becomes

$$\partial_t \mathsf{M}_n - \mathsf{M}_0 \times \mathsf{M}_n = \partial_z \mathsf{T}_n - \mathsf{M}_1 \times \mathsf{T}_n, \quad (5)$$

where $\mathsf{T}_n = [(n + 1)/(2n + 1)]\mathsf{M}_{n+1} + [n/(2n + 1)]\mathsf{M}_{n-1}$ that approximates to $\mathsf{M}_n + \partial_n \mathsf{M}_n/(2n + 1) + \partial_n^2 \mathsf{M}_n/2$ in the continuum limit of the discrete variable $n$ [9]. After dotting Eq. (5) with $\mathsf{M}_n$ and averaging over $\Delta r$, assuming it distributes over other operations, one finds for large $n$:

$$\partial_t \langle M_n \rangle = \frac{\langle M_1 \rangle}{2} \left( \partial_n^2 \langle M_n \rangle + \frac{1}{n} \partial_n \langle M_n \rangle \right). \quad (6)$$

The full derivation is given in the Supplemental Material [46]. Here $\langle M_n \rangle$ denotes the spatially coarse-grained value of $M_n = |\mathsf{M}_n|$. Equation (6) is a diffusion-advection equation where $n$ plays the role of space and $\langle M_1 \rangle$ of the diffusion constant. $G_v$ and initial conditions for $\mathsf{S}_v$ are smooth in $v$, so that $\langle M_n \rangle$ are initially small for $n \gg 1$. As time passes, the system *diffuses* from low-$n$ to high-$n$ multipoles.

One can obtain an analytical solution to the above partial differential equation if $\langle M_1 \rangle$ is approximately constant. First we note that Eq. (6) remains invariant under the scaling $n \to an$ and $t \to a^2 t$ with $a > 0$. Therefore, the solution for $\langle M_n \rangle$ can depend on $n$ and $t$ only through the scaling variable $\xi = n^2/t$. Using $\xi$ as the independent variable, Eq. (6) becomes an ordinary differential equation, $2d_\xi^2 \langle M_n \rangle + (1/\langle M_1 \rangle + 2/\xi) d_\xi \langle M_n \rangle = 0$. This has a solution $\langle M_n \rangle = c_1 \mathrm{Ei}[-n^2/(2\langle M_1 \rangle t)] + c_2$, in terms of the exponential integral $\mathrm{Ei}[x] = \int_{-\infty}^x dy\, e^y/y$. This solution, valid for large $n$, predicts how each $\langle M_n \rangle$, starting at $\langle M_n \rangle^{\mathrm{ini}}$, grows exponentially, peaks at $t_n^{\mathrm{peak}} \approx n^2/(2\langle M_1 \rangle)$, and asymptotes to $\langle M_n \rangle^{\mathrm{fin}}$ at large times. The finite behavior at large $t$ is crucial to be able to truncate the multipole expansion. The solution shows that kinematic decoherence has a strong dependence on $\langle M_1 \rangle$, which is initially $1 - A/2$ for our ELNs. Thus, for small lepton asymmetry $A$ the effective diffusion coefficient $\langle M_1 \rangle$ is larger. Further, shrinking of $\langle M_1 \rangle$ results in less kinematic decoherence at later times, and as time progresses the system reaches an almost steady state with no further diffusion in multipole space. On the other hand for larger lepton asymmetry, i.e., smaller $\langle M_1 \rangle^{\mathrm{ini}}$, there is less diffusion and depolarization throughout.

To verify the above analytical solution, we numerically solve Eq. (3) for our suite of ELNs. In Fig. 3, we show an illustrative result for $\mathsf{S}_v^\parallel$, the $\langle M_1 \rangle$ for all the ELNs, and various $\langle M_n \rangle$ for $A = 0.2$. The top left panel shows how the flavor composition, even for a single $v$ mode, is scrambled within picoseconds and sub-mm distances. This timescale depends logarithmically on the initial seed but the final state is insensitive to it. In the right panel, we see $\langle M_1 \rangle$ is approximately constant at early and late epochs, but decreases at $t \approx 3.5$ ps. We will explain the decrease in just a moment, but using the approximately constant $\langle M_1 \rangle$ in our analytical solutions for $\langle M_n \rangle$, we find qualitative agreement with the numerical results shown in the bottom panel of Fig. 3. The sharp change in $\langle M_1 \rangle^{\mathrm{ini}}$ at $t \approx 3.5$ ps prevents a perfect agreement. Higher multipoles (fainter curves) rise, peak, and fall asymptotically, one-by-one, as predicted.

*Transverse relaxation.*—For the lower-$n$ multipoles, e.g., $\langle M_0 \rangle$, $\langle M_1 \rangle$, etc., the preceding discussion does not
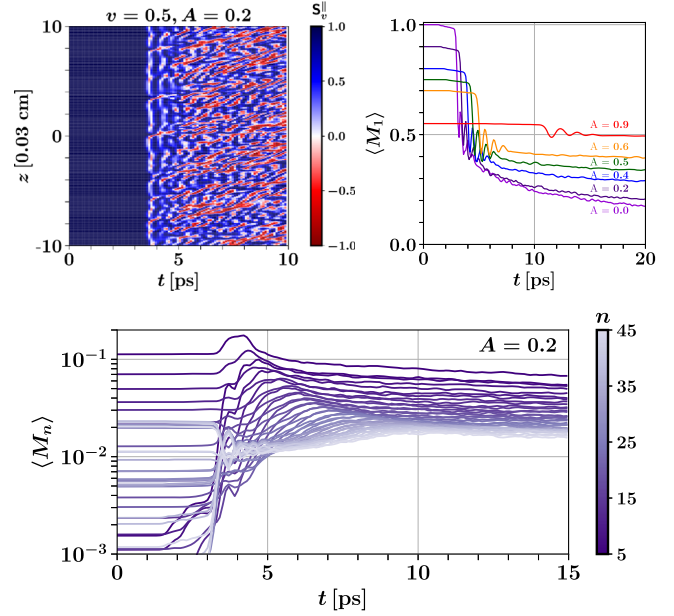


FIG. 3. Multipole diffusion: Evolution of $\mathsf{S}_v^\parallel$ for $v = 0.5$ and $A = 0.2$ (top left) and $\langle M_1 \rangle$ for various ELNs (top right). Evolution of $\langle M_n \rangle$ for large $n$ and $A = 0.2$ (bottom panel).

apply. Rather, comparing the top and bottom panels in Fig. 4, one sees that $\langle \mathsf{S}_v^\parallel \rangle$ shrinks *if* and *when* $\langle H_v^\perp \rangle \approx \langle H_v^\parallel \rangle$. We now explain this phenomenon. *Naively*, the spatial average of Eq. (3) is $d_t \langle \mathsf{S}_v \rangle = \langle \mathsf{H}_v \rangle \times \langle \mathsf{S}_v \rangle$, which can be visualized as a spin $\langle \mathsf{S}_v \rangle$ precessing around the magnetic field $\langle \mathsf{H}_v \rangle$. Note that $\mathsf{H}_v \approx -(\frac{1}{3}\mathsf{M}_0 + v\mathsf{M}_1)$ in a frame corotating with the $\mathsf{M}_0$-$\mathsf{M}_1$ plane, for our choice of
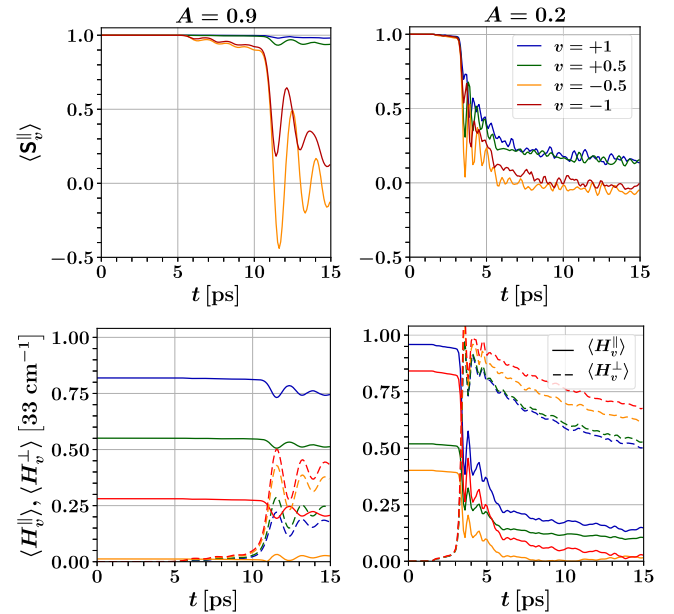


FIG. 4. Relaxation: Evolution of $\langle \mathsf{S}_v^\parallel \rangle$ for $v = \pm 1$, $\pm 0.5$ (top panels) for $A = 0.9$ (left) and $A = 0.2$ (right). $\langle H_v^\parallel \rangle$ and $\langle H_v^\perp \rangle$, in solid and dashed lines, respectively (bottom panels).

ELNs [39]. Thus the length of $\langle \mathsf{S}_v \rangle$ ought to be constant. However, the length of $\langle \mathsf{S}_v \rangle$ in fact becomes smaller. Initially, $\langle \mathsf{S}_v \rangle$ is along $\hat{\mathbf{e}}_3$, and it starts tilting away due to the action of $\mathsf{H}_\omega^{\text{vac}}$. Considering its moments, $\langle \mathsf{M}_0 \rangle$ is conserved, as $d_t \langle \mathsf{M}_0 \rangle = 0$, with $\langle \mathsf{M}_0^{\parallel} \rangle = A$. On the other hand, $\langle \mathsf{M}_1 \rangle$ has the motion of an inverted pendulum [38,39]. $\mathsf{M}_1$ tends to tip over, so that $H_v^{\parallel} = |\frac{1}{3}A + v\mathsf{M}_1^{\parallel}|$ becomes smaller as well. Eventually, when $\langle H_v^{\perp} \rangle \approx \langle H_v^{\parallel} \rangle$, the $\langle \mathsf{S}_v \rangle$ makes a large precession angle and reaches the transverse plane. At this point, the averaging procedure does not factorize and $\mathsf{S}_v$ at different spatial locations relatively dephase and their coarse-grained transverse component $\langle S_v^{\perp} \rangle$ shrinks irreversibly [39]. Thus the lengths $\langle S_v \rangle$ and $\langle M_1 \rangle$ also become smaller. This mechanism of dephasing of transverse components is familiar as *T2 relaxation* in the context of magnetic resonance imaging [47].

Figure 4 shows that the $v < 0$ modes, for which $\langle H_v^{\perp} \rangle$ overshoots $\langle H_v^{\parallel} \rangle$, are depolarized completely, so $\langle \mathsf{S}_{v<0}^{\parallel} \rangle \to 0$. For $v > 0$, the relaxation is less prominent, especially when $A$ is large. To zeroth order in $v$, one has $\langle \mathsf{S}_{v>0}^{\parallel} \rangle|^{\text{fin}} \approx A$, where we use $\langle \mathsf{S}_{v<0}^{\parallel} \rangle|^{\text{fin}} \to 0$ and enforce conservation of lepton asymmetry. For our chosen form of $G_v$, with $A > 0$ and a forward excess, it further implies that $\langle \mathsf{M}_1^{\parallel} \rangle|^{\text{fin}} \approx A/2$, as opposed to its initial value $1 - A/2$. For ELNs with a backward excess and/or $A < 0$, analogous arguments apply.

*Depolarization.*—To quantify the effect of relaxation we define the depolarization factor as the relative reduction in the length of each Bloch vector, $f_v^D = \frac{1}{2}(1 - \langle \mathsf{S}_v^{\parallel} \rangle^{\text{fin}}/\langle \mathsf{S}_v^{\parallel} \rangle^{\text{ini}})$. For flavor-pure initial conditions, $\langle \mathsf{S}_v^{\parallel} \rangle^{\text{ini}} = 1$. As noted, $f_v^D$ is 0 ($\frac{1}{2}$) when there is no (perfect) depolarization, and lies between $\frac{1}{2}$ and 1 if there is effective conversion to the other flavor.

The extent of depolarization can be readily found. For positive lepton asymmetry, $A > 0$, the negative velocity modes are almost completely depolarized, so clearly $f_{v<0}^D \approx \frac{1}{2}$. For positive velocity modes the functional behavior of $f_{v>0}^D$ can be obtained by using the multipole expansion: $G_v \mathsf{S}_v^{\parallel}|^{\text{fin}} = \frac{1}{2}\mathsf{M}_0^{\parallel}|^{\text{fin}} + \frac{3}{2}v\mathsf{M}_1^{\parallel}|^{\text{fin}} + \mathcal{O}(v^2)$, dropping the higher multipoles. As we found, $\langle \mathsf{M}_0^{\parallel} \rangle = A$ is a constant in time but $\langle \mathsf{M}_1^{\parallel} \rangle$ flips from $1 - A/2$ to $A/2$. This brings us to the promised formula for the depolarization factor that was shown in Fig. 2:

$$f_v^D \approx \begin{cases} \frac{1}{2} - \frac{A}{4} - \frac{3A}{8}v, & \text{if } v > 0, \\ \frac{1}{2}, & \text{if } v < 0, \end{cases} \tag{7}$$

dropping the higher multipoles. For ELNs with a backward excess and/or $A < 0$ the analogous formula for $f_v^D$ is easy

to obtain using the mirror symmetries $+v \leftrightarrow -v$ and $+G_v^{(A<0)} \leftrightarrow -G_{-v}^{(A>0)}$ and a rescaling of $\mu_0$ [39].

*Summary and outlook.*—We have presented an analytical theory of fast neutrino flavor conversions in the nonlinear regime. We showed *how*, as time passes, flavor differences over large ranges of velocity diffuse into variations over smaller velocity ranges, or equivalent ranges of emission angles, causing depolarization. Coarse-graining, by averaging over a small spatial volume and over small ranges of $v$, introduces loss of information that leads to an apparent arrow of time out of the time-reversible Eq. (2). $f_v^D$ used in Eq. (1) must be understood in a spatially averaged sense. These features, including both $v > 0$ and $v < 0$ modes, are carefully verified using our state-of-the-art numerics [39]. In contrast, without nonlinearity or coarse-graining no irreversible depolarization occurs and one finds wave solutions [37]. We then showed that the epoch of T2 relaxation determines *when* depolarization occurs, and the initial lepton asymmetry $A$ determines the rate of flavor depolarization. Finally, we gave a strategy and a formula for computing the extent of depolarization, which is the ultimate outcome for fast collective oscillations pointed out by Sawyer [24–26].

Like the Landau-Zener formula [48–51], strictly applicable for a linearly varying density at a Mikheyev-Smirnov-Wolfenstein resonance [52,53], our depolarization formula gives a simple formula for the chosen class of ELNs. Both need further generalization in real-world applications. A difference is that depolarization, as long as it occurs, is irreversible. This final "thermalized" state is insensitive to microscopic details, e.g., the different purple lines in Fig. 2 are for different initial seeds, depending only on conserved quantities like $A$. See the Supplemental Material [46]. The key insight is to identify the role of coarse-graining and relaxation, which leads to this universal behavior.

The neutrino flux after suffering fast conversions can be determined using the depolarization factor $f_v^D$. In a SN, these fluxes are responsible for heating and cooling processes [54]. The net heating rate $\dot{Q}$ that is responsible for shock revival depends on the product of cross section $\sigma_\alpha \propto E_\alpha^2$ and luminosity $L_\alpha \propto v E_\alpha F_\alpha$, with the $\bar{\nu}_e$ and $\nu_e$ dominating owing to their larger cross sections [55]. It is clear that depolarization can change $\dot{Q}$, because $\bar{\nu}_e$ and $\nu_e$ energies move closer to that of $\nu_x$, and the increase proportional to $E_{\nu_x}^3/E_{\bar{\nu}_e}^3$ can be quite large [56]. Including the effects of subsequent slow collective oscillations [7,14], MSW conversions, propagation and earth effects [57], allows one to determine the final neutrino signal from a SN explosion. These can be measured at current and upcoming neutrino telescopes and may provide a remarkable way to directly test neutrino-neutrino interactions [58–60]. These standard model interactions have never been directly tested in a laboratory. Of course, a variety of other particle physics and astrophysics information may be

gleaned from such a signal [61–68]. In many such analyses, knowing $f_v^D$ is important. For the first time, our work provides this crucial input.

What lies ahead? For the more exciting, one could use this setup as a test of possible secret neutrino-neutrino interactions [69], that have been proposed as a solution to the Hubble tension [70,71]. Collective flavor conversions may also occur in the disk of merging neutron stars [13,72,73]. These possibilities are not yet fully explored. Sticking to basics, however, several improvements, extensions, and applications are possible. Three-flavor effects were ignored here [12,34,74,75]. It will be interesting to see if our approach can be extended to include higher order terms in $v$ and $A$, break the azimuthal symmetry, and include more complicated ELNs. These are important, but will not qualitatively change the picture we painted. As regards experiments, the diffuse SN neutrino background may soon become detectable [76,77], and hopefully the next galactic SN is not too far in the future [78–80]. These effects may also have observable impact on the neutron star merger events at LIGO [81]. It is therefore of paramount importance that predictions for neutrinos are put on a firm footing and the experiments are well prepared [82,83], so that we can reliably extract all the physics out of these once-in-a-lifetime events.

---

[*]soumyaquanta@gmail.com
[†]bdasgupta@theory.tifr.res.in

[1] S. Strogatz, Sync: How order emerges from chaos in the universe, nature, and daily life, Hyperion, 2012.
[2] J. T. Pantaleone, Dirac neutrinos in dense matter, Phys. Rev. D **46**, 510 (1992).
[3] V. A. Kostelecky and S. Samuel, Selfmaintained coherent oscillations in dense neutrino gases, Phys. Rev. D **52**, 621 (1995).
[4] S. Pastor, G. G. Raffelt, and D. V. Semikoz, Physics of synchronized neutrino oscillations caused by selfinteractions, Phys. Rev. D **65**, 053011 (2002).
[5] A. Friedland and C. Lunardini, Neutrino flavor conversion in a neutrino background: Single particle versus multi-particle description, Phys. Rev. D **68**, 013007 (2003).
[6] N. F. Bell, A. A. Rawlinson, and R. Sawyer, Speedup through entanglement: Many body effects in neutrino processes, Phys. Lett. B **573**, 86 (2003).
[7] H. Duan, G. M. Fuller, J. Carlson, and Y.-Z. Qian, Simulation of coherent non-linear neutrino flavor transformation in the supernova environment. 1. correlated neutrino trajectories, Phys. Rev. D **74**, 105014 (2006).
[8] S. Hannestad, G. G. Raffelt, G. Sigl, and Y. Y. Wong, Self-induced conversion in dense neutrino gases: Pendulum in flavour space, Phys. Rev. D **74**, 105010 (2006).
[9] G. Raffelt and G. Sigl, Self-induced decoherence in dense neutrino gases, Phys. Rev. D **75**, 083002 (2007).
[10] G. G. Raffelt and A. Y. Smirnov, Self-induced spectral splits in supernova neutrino fluxes, Phys. Rev. D **76**, 081301(R) (2007).
[11] A. Esteban-Pretel, S. Pastor, R. Tomas, G. G. Raffelt, and G. Sigl, Decoherence in supernova neutrino transformations suppressed by deleptonization, Phys. Rev. D **76**, 125018 (2007).
[12] B. Dasgupta and A. Dighe, Collective three-flavor oscillations of supernova neutrinos, Phys. Rev. D **77**, 113002 (2008).
[13] B. Dasgupta, A. Dighe, A. Mirizzi, and G. G. Raffelt, Collective neutrino oscillations in non-spherical geometry, Phys. Rev. D **78**, 033014 (2008).
[14] B. Dasgupta, A. Dighe, G. G. Raffelt, and A. Y. Smirnov, Multiple Spectral Splits of Supernova Neutrinos, Phys. Rev. Lett. **103**, 051105 (2009).
[15] A. Friedland, Self-Refraction of Supernova Neutrinos: Mixed Spectra and Three-Flavor Instabilities, Phys. Rev. Lett. **104**, 191102 (2010).
[16] Y. Pehlivan, A. Balantekin, T. Kajino, and T. Yoshida, Invariants of collective neutrino oscillations, Phys. Rev. D **84**, 065008 (2011).
[17] S. Chakraborty, A. Mirizzi, N. Saviano, and D. d. S. Seixas, Suppression of the multi-azimuthal-angle instability in dense neutrino gas during supernova accretion phase, Phys. Rev. D **89**, 093001 (2014).
[18] G. Mangano, A. Mirizzi, and N. Saviano, Damping the neutrino flavor pendulum by breaking homogeneity, Phys. Rev. D **89**, 073017 (2014).
[19] H. Duan and S. Shalgar, Flavor instabilities in the neutrino line model, Phys. Lett. B **747**, 139 (2015).
[20] B. Dasgupta and A. Mirizzi, Temporal instability enables neutrino flavor conversions deep inside supernovae, Phys. Rev. D **92**, 125030 (2015).
[21] S. Birol, Y. Pehlivan, A. Balantekin, and T. Kajino, Neutrino spectral split in the exact many body formalism, Phys. Rev. D **98**, 083002 (2018).
[22] R. S. Hansen and A. Y. Smirnov, Effect of extended $\nu$ production region on collective oscillations in supernovae, J. Cosmol. Astropart. Phys. 10 (2019) 027.
[23] M. J. Cervia, A. V. Patwardhan, A. Balantekin, d. S. Coppersmith, and C. W. Johnson, Entanglement and collective flavor oscillations in a dense neutrino gas, Phys. Rev. D **100**, 083001 (2019).
[24] R. Sawyer, Speed-up of neutrino transformations in a supernova environment, Phys. Rev. D **72**, 045003 (2005).
[25] R. Sawyer, The multi-angle instability in dense neutrino systems, Phys. Rev. D **79**, 105003 (2009).

[26] R. F. Sawyer, Neutrino Cloud Instabilities Just Above the Neutrino Sphere of a Supernova, Phys. Rev. Lett. 116, 081101 (2016).

[27] S. Chakraborty, R. S. Hansen, I. Izaguirre, and G. Raffelt, Self-induced neutrino flavor conversion without flavor mixing, J. Cosmol. Astropart. Phys. 03 (2016) 042.

[28] B. Dasgupta, A. Mirizzi, and M. Sen, Fast neutrino flavor conversions near the supernova core with realistic flavor-dependent angular distributions, J. Cosmol. Astropart. Phys. 02 (2017) 019.

[29] I. Izaguirre, G. Raffelt, and I. Tamborra, Fast Pairwise Conversion of Supernova Neutrinos: A Dispersion-Relation Approach, Phys. Rev. Lett. 118, 021101 (2017).

[30] F. Capozzi, B. Dasgupta, E. Lisi, A. Marrone, and A. Mirizzi, Fast flavor conversions of supernova neutrinos: Classifying instabilities via dispersion relations, Phys. Rev. D 96, 043016 (2017).

[31] B. Dasgupta and M. Sen, Fast neutrino flavor conversion as oscillations in a quartic potential, Phys. Rev. D 97, 023017 (2018).

[32] T. Morinaga and S. Yamada, Linear stability analysis of collective neutrino oscillations without spurious modes, Phys. Rev. D 97, 023024 (2018).

[33] B. Dasgupta, A. Mirizzi, and M. Sen, Simple method of diagnosing fast flavor conversions of supernova neutrinos, Phys. Rev. D 98, 103001 (2018).

[34] S. Airen, F. Capozzi, S. Chakraborty, B. Dasgupta, G. Raffelt, and T. Stirner, Normal-mode analysis for collective neutrino oscillations, J. Cosmol. Astropart. Phys. 12 (2018) 019.

[35] S. Abbar and M. C. Volpe, On fast neutrino flavor conversion modes in the nonlinear regime, Phys. Lett. B 790, 545 (2019).

[36] F. Capozzi, G. Raffelt, and T. Stirner, Fast neutrino flavor conversion: Collective motion vs. decoherence, J. Cosmol. Astropart. Phys. 09 (2019) 002.

[37] J. D. Martin, C. Yi, and H. Duan, Dynamic fast flavor oscillation waves in dense neutrino gases, Phys. Lett. B 800, 135088 (2020).

[38] L. Johns, H. Nagakura, G. M. Fuller, and A. Burrows, Neutrino oscillations in supernovae: Angular moments and fast instabilities, Phys. Rev. D 101, 043009 (2020).

[39] S. Bhattacharyya and B. Dasgupta, Fast neutrino flavor conversion at late time, Phys. Rev. D 102, 063018 (2020).

[40] I. Tamborra, L. Huedepohl, G. Raffelt, and H.-T. Janka, Flavor-dependent neutrino angular distribution in core-collapse supernovae, Astrophys. J. 839, 132 (2017).

[41] F. Capozzi, B. Dasgupta, A. Mirizzi, M. Sen, and G. Sigl, Collisional Triggering of Fast Flavor Conversions of Supernova Neutrinos, Phys. Rev. Lett. 122, 091101 (2019).

[42] S. Shalgar and I. Tamborra, On the occurrence of crossings between the angular distributions of electron neutrinos and antineutrinos in the supernova core, Astrophys. J. 883, 80 (2019).

[43] T. Morinaga, H. Nagakura, C. Kato, and S. Yamada, Fast neutrino-flavor conversion in the preshock region of core-collapse supernovae, Phys. Rev. Research 2, 012046(R) (2020).

[44] S. Abbar, H. Duan, K. Sumiyoshi, T. Takiwaki, and M. C. Volpe, Fast neutrino flavor conversion modes in multi-dimensional core-collapse supernova models: The role of the asymmetric neutrino distributions, Phys. Rev. D 101, 043016 (2020).

[45] R. Glas, H. T. Janka, F. Capozzi, M. Sen, B. Dasgupta, A. Mirizzi, and G. Sigl, Fast neutrino flavor instability in the neutron-star convection layer of three-dimensional supernova models, Phys. Rev. D 101, 063001 (2020).

[46] See Supplemental Material at http://link.aps.org/supplemental/10.1103/PhysRevLett.126.061302 for derivations of Eqs. (5) and (6), details of numerical methods employed, and the role of seeds for triggering the flavor evolution.

[47] D. B. Plewes and W. Kucharczyk, Physics of MRI: A primer, J. Magn. Reson. Imaging 35, 1038 (2012).

[48] L. D. Landau, Zur Theorie der Energieubertragung. II, Phys. Z. Sowjetunion 2, 46 (1932).

[49] E. Majorana, Oriented atoms in a variable magnetic field, Nuovo Cimento 9, 43 (1932).

[50] E. C. G. Stueckelberg, Theorie der unelastischen Stoesse zwischen Atomen, Helv. Phys. Acta 5, 369 (1932).

[51] C. Zener, Nonadiabatic crossing of energy levels, Proc. R. Soc. A 137, 696 (1932).

[52] L. Wolfenstein, Neutrino oscillations in matter, Phys. Rev. D 17, 2369 (1978).

[53] S. P. Mikheev and A. Yu. Smirnov, Neutrino oscillations in an inhomogeneous medium: Adiabatic regime, Sov. Phys. JETP 65, 230 (1987).

[54] S. A. Colgate and R. H. White, The hydrodynamic behavior of Supernovae explosions, Astrophys. J. 143, 626 (1966).

[55] H. T. Janka, Conditions for shock revival by neutrino heating in core collapse supernovae, Astron. Astrophys. 368, 527 (2001).

[56] B. Dasgupta, E. P. O'Connor, and C. D. Ott, The role of collective neutrino flavor oscillations in core-collapse supernova shock revival, Phys. Rev. D 85, 065008 (2012).

[57] A. S. Dighe and A. Yu. Smirnov, Identifying the neutrino mass spectrum from the neutrino burst from a supernova, Phys. Rev. D 62, 033007 (2000).

[58] A. G. Rosso, F. Vissani, and M. C. Volpe, What can we learn on supernova neutrino spectra with water Cherenkov detectors?, J. Cosmol. Astropart. Phys. 04 (2018) 040.

[59] S. Seadrow, A. Burrows, D. Vartanyan, D. Radice, and M. A. Skinner, Neutrino signals of core-collapse supernovae in underground detectors, Mon. Not. R. Astron. Soc. 480, 4710 (2018).

[60] F. Capozzi, B. Dasgupta, and A. Mirizzi, Model-independent diagnostic of self-induced spectral equalization versus ordinary matter effects in supernova neutrinos, Phys. Rev. D 98, 063013 (2018).

[61] S. Horiuchi and J. P. Kneller, What can be learned from a future supernova neutrino detection?, J. Phys. G 45, 043002 (2018).

[62] C. Simpson et al. (Super-Kamiokande Collaboration), Sensitivity of super-Kamiokande with gadolinium to low energy anti-neutrinos from pre-supernova emission, Astrophys. J. 885, 133 (2019).

[63] S. Horiuchi, K. Nakamura, T. Takiwaki, and K. Kotake, Estimating the core compactness of massive stars with Galactic supernova neutrinos, J. Phys. G 44, 114001 (2017).

[64] Y. Yang and J. P. Kneller, Neutrino flavor transformation in supernovae as a probe for nonstandard neutrino-scalar interactions, Phys. Rev. D **97,** 103018 (2018).

[65] A. Gallo Rosso, S. Abbar, F. Vissani, and M. C. Volpe, Late time supernova neutrino signal and proto-neutron star radius, J. Cosmol. Astropart. Phys. 12 (2018) 006.

[66] J. F. Cherry, G. M. Fuller, S. Horiuchi, K. Kotake, T. Takiwaki, and T. Fischer, Time of flight and supernova progenitor effects on the neutrino halo, Phys. Rev. D **102,** 023022 (2020).

[67] H. Ko *et al.*, Neutrino process in core-collapse supernovae with neutrino self-interaction and MSW effects, Astrophys. J. Lett. **891,** L24 (2020).

[68] A. de Gouvea, I. J. M. Soler, Y. F. Perez-Gonzalez, and M. Sen, Fundamental physics with the diffuse supernova background neutrinos, Phys. Rev. D **102,** 123012 (2020).

[69] A. Dighe and M. Sen, Nonstandard neutrino self-interactions in a supernova and fast flavor conversions, Phys. Rev. D **97,** 043011 (2018).

[70] F.-Y. Cyr-Racine and K. Sigurdson, Limits on neutrino-neutrino scattering in the early Universe, Phys. Rev. D **90,** 123533 (2014).

[71] M. Archidiacono and S. Hannestad, Updated constraints on non-standard neutrino interactions from Planck, J. Cosmol. Astropart. Phys. 07 (2014) 046.

[72] M.-R. Wu, I. Tamborra, O. Just, and H.-T. Janka, Imprints of neutrino-pair flavor conversions on nucleosynthesis in ejecta from neutron-star merger remnants, Phys. Rev. D **96,** 123015 (2017).

[73] I. Padilla-Gay, S. Shalgar, and I. Tamborra, Multi-dimensional solution of fast neutrino conversions in binary neutron star merger remnants, J. Cosmol. Astropart. Phys. 01 (2021) 017.

[74] M. Chakraborty and S. Chakraborty, Three flavor neutrino conversions in supernovae: Slow & fast instabilities, J. Cosmol. Astropart. Phys. 01 (2020) 005.

[75] F. Capozzi, M. Chakraborty, S. Chakraborty, and M. Sen, Fast flavor conversions in supernovae: The rise of mu-tau neutrinos, Phys. Rev. Lett. **125,** 251801 (2020).

[76] J. F. Beacom and M. R. Vagins, GADZOOKS! Anti-Neutrino Spectroscopy with Large Water Cherenkov Detectors, Phys. Rev. Lett. **93,** 171101 (2004).

[77] D. Castelvecchi, Gigantic Japanese detector prepares to catch neutrinos from supernovae, Nature (London) **566,** 438 (2019).

[78] K. Abe *et al.* (Super-Kamiokande Collaboration), Real-time supernova neutrino burst monitor at super-Kamiokande, Astropart. Phys. **81,** 39 (2016).

[79] Yu. F. Novoseltsev, M. M. Boliev, V. I. Volchenko, G. V. Volchenko, I. M. Dzaparova, M. M. Kochkarov, R. V. Novoseltseva, V. B. Petkov, and A. F. Yanin, Searching for neutrino bursts in the galaxy: 36 years of exposure, J. Exp. Theor. Phys. **125,** 73 (2017).

[80] B. Abi *et al.* (DUNE Collaboration), Supernova neutrino burst detection with the deep underground neutrino experiment, arXiv:2008.06647.

[81] B. Abbott *et al.* (LIGO Scientific, Virgo, Fermi GBM, INTEGRAL, IceCube, AstroSat Cadmium Zinc Telluride Imager Team, IPN, Insight-Hxmt, ANTARES, Swift, AGILE Team, 1M2H Team, Dark Energy Camera GW-EM, DES, DLT40, GRAWITA, Fermi-LAT, ATCA, AS-KAP, Las Cumbres Observatory Group, OzGrav, DWF (Deeper Wider Faster Program), AST3, CAASTRO, VINROUGE, MASTER, J-GEM, GROWTH, JAGWAR, CaltechNRAO, TTU-NRAO, NuSTAR, Pan-STARRS, MAXI Team, TZAC Consortium, KU, Nordic Optical Telescope, ePESSTO, GROND, Texas Tech University, SALT Group, TOROS, BOOTES, MWA, CALET, IKI-GW Follow-up, H.E.S.S., LOFAR, LWA, HAWC, Pierre Auger, ALMA, Euro VLBI Team, Pi of Sky, Chandra Team at McGill University, DFN, ATLAS Telescopes, High Time Resolution Universe Survey, RIMAS, RATIR, SKA South Africa/MeerKAT Collaboration), Multi-messenger observations of a binary neutron star merger, Astrophys. J. Lett. **848,** L12 (2017).

[82] A. Friedland and S. W. Li, Understanding the energy resolution of liquid argon neutrino detectors, Phys. Rev. D **99,** 036009 (2019).

[83] S. W. Li, L. F. Roberts, and J. F. Beacom, Exciting prospects for detecting late-time neutrinos from core-collapse supernovae, arXiv:2008.04340 [Phys. Rev. D (to be published)].